When $x<0$ we must close the contour in the upper half plane and when $x>0$ in the lower half plane. Hence

$$K_0(x)=\begin{cases}K^+(x) & x<0\\ K^-(x) & x>0\end{cases} \tag{18}$$

where $K^{\pm}(x)\equiv\pm\sum$ Res in $\binom{\text{upper}}{\text{lower}}$ half plane.

Then upon evaluating the residues we find that

$$K^+(x)=\frac{1}{2i}\lim_{y\to 0}\frac{\partial}{\partial y}\times\sum_{n=-\infty}^{\infty}\frac{(\Gamma_n-\alpha_n^+ s^\dagger)e^{-i[(\alpha_n^+-Mk)x+(\Gamma_n-\alpha_n^+ s^\dagger)y/s]}}{(\alpha_n^+-k/M)\ (s^\dagger\Gamma_n-d^{\dagger 2}\alpha_n^+)} \tag{19}$$

and

$$K^-(x)=\frac{\omega}{2}\ \frac{\sinh(\omega s)\ e^{i\omega x}}{\cosh(\omega s)-\cos(\sigma-s\dagger\omega)}-\frac{1}{2i}\lim_{y\to 0}\frac{\partial}{\partial y}\times\sum_{n=-\infty}^{\infty}\frac{(\Gamma_n-\alpha_n^- s^\dagger)\ e^{-i[(\alpha_n^- -Mk)x+(\Gamma_n-\alpha_n^- s^\dagger)y/s]}}{(\alpha_n^- -k/M)\ (s^\dagger\Gamma_n-d^{\dagger 2}\alpha_n^-)} \tag{20}$$

These series are only conditionally convergent and will not converge at all if we take the derivative term by term. To obtain convergent series, notice that since $\alpha_n^{\pm}\sim\Gamma_n/(s^\dagger\pm\beta s)+0(n^{-1})$ as $n\to\infty$ the nth term of these sums behave like

$$\left\{\exp\left[-i\Gamma_n\left(\frac{x\pm\beta y}{s^\dagger\pm\beta s}\right)\right]\right\}/\Gamma_n$$

The series composed of these terms will converge to a row of step functions. Hence, its derivative will converge to a row of delta functions. We can evaluate the latter series by using the theory of distributions to show that[3]

$$\lim_{y\to 0}\frac{\partial}{\partial y}\sum_{n=-\infty}^{\infty}\frac{1}{\Gamma_n}e^{-i\Gamma_n(x\mp\beta y)/(s^\dagger\pm\beta s)}=\pm\frac{i\beta}{s^\dagger\pm\beta s}e^{i[(\sigma-Mks^\dagger)/(s^\dagger\pm\beta s)]x}\sum_{n=-\infty}^{\infty}e^{-(2in\pi x)/(s^\dagger\pm\beta s)}$$

$$=\pm i\beta\sum_{n=-\infty}^{\infty}e^{in(\sigma-Mks^\dagger)}\delta(x_n\pm\beta sn)$$

Hence

$$K^{\pm}(x)=\tilde{K}^{\pm}(x)+\frac{\beta}{2}\sum_{n=-\infty}^{\infty}e^{i(n\sigma+Mkx_n)}\delta(x_n\pm\beta sn) \tag{21}$$

where

$$\tilde{K}^+\equiv-\frac{e^{iMkx}}{2s}\sum_{n=-\infty}^{\infty}\left[\frac{(\Gamma_n-\alpha_n^+ s^\dagger)^2 e^{-i\alpha_n^+ x}}{(\alpha_n^+-k/M)(s^\dagger\Gamma_n-d^{\dagger 2}\alpha_n^+)}+\frac{s\beta e^{-i\Gamma_n x/(s^\dagger-\beta s)}}{s^\dagger-\beta s}\right]$$

and

$$\tilde{K}^-\equiv\frac{\omega\sinh(\omega s)\ e^{i\omega x}}{2[\cosh(\omega s)-\cos(\sigma-s^\dagger\omega)]}+\frac{e^{iMkx}}{2s}\sum_{n=-\infty}^{\infty}\left[\frac{(\Gamma_n-\alpha_n^- s^\dagger)^2 e^{-i\alpha_n^- x}}{(\alpha_n^- -k/M)(s^\dagger\Gamma_n-d^{\dagger 2}\alpha_n^-)}-\frac{s\beta e^{-i\Gamma_n x/(s^\dagger+\beta s)}}{s^\dagger+\beta s}\right]$$

are now convergent series. The kernel function is given by Eqs. (18) and (21). Only a finite number of the infinite row of delta functions in Eq. (21) will contribute to the integral in Eq. (13). However when this kernel is substituted into Eq. (13), we obtain a functional integral equation (and not an ordinary integral equation) due to the introduction of terms of the form $[P(x_n+ns\beta)]$ caused by the integration over the delta functions.

The series which appear in $\tilde{K}^{\pm}$ are only conditionally convergent. But the same device that was used to make the original series converge can also be used to render these latter series absolutely convergent. This removal of the slowly convergent part of the series results in a row of step functions which explicitly exhibit the discontinuities of $\tilde{K}^{\pm}$ (and occur at the points $x_n=\pm\beta sn$). The remaining series will represent continuous functions and will be quite suitable for numerical computation.

References

[1] Kurosaka, M., "On the Unsteady Supersonic Cascade with a Subsonic Leading Edge—An Exact Order Theory—Part 1 and 2," *Transactions of ASME, Series A, Journal of Engineering for Power*, Vol. 96, Jan. 1974, pp. 13-31.

[2] Verdon, J. M., "The Unsteady Aerodynamics of a Finite Supersonic Cascade with Subsonic Axial Flow," *Transactions of ASME, Series E, Journal of Applied Mechanics*, Vol. 40, Sept. 1973, pp. 667-671.

[3] Lighthill, M. J., *Fourier Analysis and Generalized Functions*, Cambridge University Press, New York, 1958, p. 67.

Mixing Length in Low Reynolds Number Compressible Turbulent Boundary Layers

D. M. Bushnell,* A.M. Cary Jr.,† and B. B. Holley‡
NASA Langley Research Center, Hampton, Va.

Nomenclature

C_f = skin friction coefficient, $\tau_w/1/2\,\rho_e u_e^2$
ℓ = mixing length
M = Mach number
N = power law velocity exponent, Eq. (1)
R_θ = Reynolds number based on momentum thickness
T = temperature
u = velocity
u_τ = friction velocity, $(\tau/\rho)^{1/2}$
y = normal coordinate
$\rho\overline{u'v'}$ = Reynolds stress
δ = velocity boundary-layer thickness
τ = shear stress
ρ = density
γ = ratio of specific heats
δ^+ = $\delta(u_{\tau,w}\rho_w/\mu_w)$
μ = viscosity

Subscripts

m = maximum value, evaluated herein at $y/\delta=0.5$
e = edge
w = wall
t = stagnation

Received January 27, 1975; revision received March 27, 1975.

Index categories: Boundary Layers and Convective Heat Transfer—Turbulent; Nozzle and Channel Flow; Supersonic and Hypersonic Flow.

*Head, Fluid Mechanics Branch, High-Speed Aerodynamics Division.

†Head, Applied Fluid Mechanics Section, High-Speed Aerodynamics Division. Member AIAA.

‡Mathematician, Applied Fluid Mechanics Section, High-Speed Aerodynamics Division.

SEVERAL investigators have shown that the mixing length parameter $(\ell/\delta)_m$ is larger than the accepted high Reynolds number value of 0.07-0.09 in the outer region of low Reynolds number boundary layers. This is true both for low-speed[1-4] and high-speed flow.[5,6] In earlier low-speed flow research,[1-3] $(\ell/\delta)_m$ was correlated as a function of R_θ (for zero pressure gradient). Further, Ref. 5 indicates that both the low-speed and high-speed low Reynolds number data (up to $M \simeq 20$), can be correlated using δ^+. Reference 4 used a δ^+ parameter based on the maximum shear stress in the boundary layer to correlate low Reynolds number effects in low-speed flow with and without wall blowing.

The purpose of the present Note is to re-examine the question of low Reynolds number effects in high-speed turbulent boundary layers, and in particular, to determine whether low Reynolds number amplification of shear stress is a result of transitional flow structure. Because of the extreme dearth of $(\ell/\delta)_m$ values in high-speed flows (for both high and low Reynolds numbers), a simple analysis is used herein to obtain sufficient $(\ell/\delta)_m$ values for evaluation of the low Reynolds number influence. This type of analysis was suggested by two previous investigations.[7,8] In Ref. 7, mean velocity profiles downstream of transition (up to 80-200 boundary-layer thicknesses past the nominal "end" of transition) exhibit an "overshoot" in the "N power," and this overshoot may be related to the increase in $(\ell/\delta)_m$ noted in Ref. 5 for low Reynolds number flows. In addition, Ref. 8 indicates for flat plate type flows that τ/τ_w is a unique function of y/δ for the Mach number and Reynolds number range where data are available.

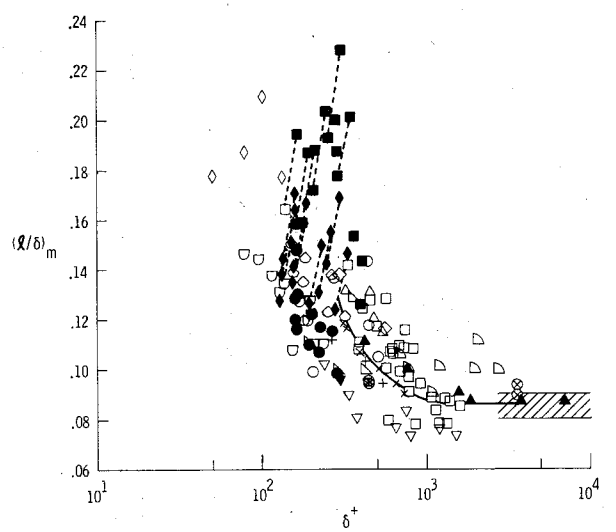

Fig. 1 Variation of mixing length with δ^+ for outer region of low Reynolds number boundary layers downstream of natural transition on plates, cones, and cylinders. See Table 1 for legend.

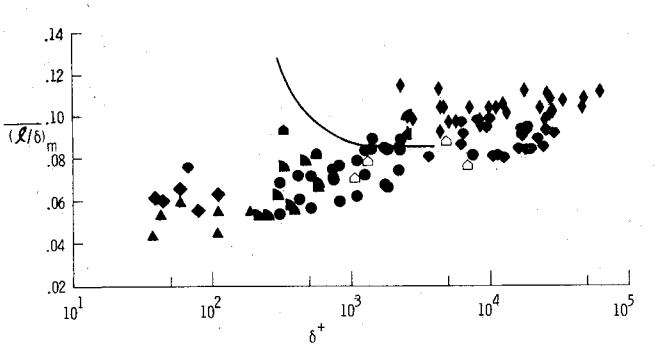

Fig. 2 Variation of mixing length with δ^+ for outer region of low Reynolds number boundary layers on nozzle walls without laminarization—retransition. See Table 1 for legend.

Table 1 Identification of data used on Figs. 1 and 2

Symbol	M	$T_w/T_{t,e}$	γ	Ref.	Author
		Data used on Fig. 1 (flat plate, cone, cylinder)			
◇	7.5-16.6	1.0	1.66	40,41 of Ref. 7	Maddalon/Henderson
●	4.9-5.2	0.56-0.87	1.4	16 of Ref. 7	Winkler/Cha
■	6.4-6.7	0.84-0.86	1.66	11	Fischer/Maddalon
○ □	6.21-6.5	0.31-0.46	1.4	14*	Keener/Hopkins
◇	5.8-7.7	0.23-0.44	1.4	13*	Hopkins/Keener
△	3.1	0.93	1.4	45 of Ref. 7	Bradfield et al.
▽	2.4	0.95-1.3	1.4	28 of Ref. 7	Higgins/Pappas
◁	2.82	0.94-1.35	1.4	33 of Ref. 7	Monagham/Cooke
▷	2.2	0.92	1.4	38 of Ref. 7	Allen/Monta
○	0→5	≈1	1.4	12 of Ref. 5	Maise/McDonald
▲	low speed	≈1	1.4	3	Simpson
▼	6.5	0.48	1.4	36 of Ref. 5	Danberg
◆	4.69-9.83	0.56-0.91	1.4	20,21,22 of Ref.7	Deem
◇	6.3-6.6	0.46-0.85	1.4	14,15 of Ref. 7	Danberg
◇	9.1-10.2	1	1.66	10*	Watson et al.
▽	3.93	0.88-0.93	1.4	11*	Hastings/Sawyer
+ x	low speed	≈1	1.4	4	Baker/Launder
▨	1.5-4.5	0.9-1	1.4	17	Sivasegaram/Whitelaw
——	low speed	≈1	1.4	1	McDonald
		Data used on Fig. 2 (nozzle wall)			
⌂	.55-3.5	0.96-0.98	1.4	18	Squire
●	5.9-10.1	0.27-0.66	1.4	92 of Ref. 7	Matthews/Trimmer
◪	5.76	0.73	1.4	30 of Ref. 5	Jones/Feller
■	10.65	0.26	1.4	31 of Ref. 5	Perry
◆	12	0.29	1.4	32 of Ref. 5	Fiore
◆	8.2-10	0.42-0.49	1.4	86 of Ref. 7	Hill
▲	6.4-11.5	0.26-0.4	1.4	9 of Ref. 7	Scaggs
—— (for Ref. w/Fig. 1 only)	low speed	≈1	1.4	1	McDonald
◣	4.9-8.2	0.46-0.92	1.4	65 of Ref. 7	Lobb et al.
◪	19.3-19.7	0.16-0.18	1.4	15	Beckwith et al.
◆	1.95-4.92	0.87-1.15	1.4	85 of Ref. 7	Thomke/Roshko
◆	0.2-2.8	0.93-1.0	1.4	16*	Winter/Gaudet

*Skin friction balance data available.

Note: Other C_f values obtained by authors either from velocity slope at the wall or momentum balance; where author gave no C_f value, it was calculated from Spalding-Chi (Ref. 22) based on R_θ (if the survey station was too close to the end of transition for the C_f prediction to be valid, a spread of 40% above the calculated C_f was used to represent the limits of C_f increase due to the proximity of transition, Ref. 23. These cases are represented by like symbols connected by a dashed line in Fig. 1).

The present approach therefore uses N power data and assumes a linear shear stress distribution (which agrees quite well with the data of Ref. 8 near the mid region of the boundary layer) to deduce $(\ell/\delta)_m$ for mean profiles. The starting points of the analysis are the following statements

$$u/u_e = (y/\delta)^{1/N} \tag{1}$$

and

$$\tau = \tau_w(1-y/\delta) \simeq \overline{\rho u'v'} \simeq \rho(\ell/\delta)_m{}^2 u_e{}^2 \left[\frac{\partial(u/u_e)}{\partial(y/\delta)}\right]^2 \tag{2}$$

If we use Eq. (1) in Eq. (2), along with a linear or quadratic total temperature-velocity relationship (linear used for flat plate, quadratic used for nozzle walls, which is generally correct as shown in Ref. 9) there result the following expressions for $(\ell/\delta)_m$ (valid near the mid region of $dp/dx \simeq 0$ boundary layers, $y/\delta \simeq 0.4$-0.6)

$$(\ell/\delta)_m = \left[\frac{\mathfrak{A}}{\mathfrak{B}}\right]^{1/2} \tag{3}$$

where

$$\mathfrak{A} = \frac{Cf}{2}(1-y/\delta)N^2\left\{(y/\delta)^{J/N}(1-T_w/T_{t,e}) + T_w/T_{t,e} - (y/\delta)^{2/N}\left[1-1/\left(1+\frac{\gamma-1}{2}M_e^2\right)\right]\right\}$$

and $J=1$ for linear T_t-u and 2 for quadratic T_t-u

$$\mathfrak{B} = (y/\delta)^{2-2N/N}\left[1/\left(1+\frac{\delta-1}{2}M_e^2\right)\right]$$

where $(\ell/\delta)_m$ is a $f(C_f/2, N, T_w/T_t, \gamma, \text{and } M_e)$

Initial calculations showed that $(\ell/\delta)_m$ values computed from Eq. (3) have a gentle peak near $y/\delta \simeq 0.5$ and generally decrease for y/δ values less than or greater than 0.5; thus results shown herein are at $y/\delta = 0.5$. Values of $(\ell/\delta)_m$ were computed for those investigations where mean flow profiles are available, and C_f is either given or can be computed with

reasonable accuracy. Such data available before $\simeq$ 1970 are given in Ref. 7, while most of the pertinent data since 1970 are given in Refs. 10-16.

The computed $(\ell/\delta)_m$ values, along with $(\ell/\delta)_m$ results available in the literature,[1,4,5,17,18] are shown on Figs. 1 and 2. Table 1 identifies the data used. Because it was suspected that the low Reynolds number amplification is connected with the residue of a transition process,[7] the data were broken down into 2 categories. Category 1 (Fig. 1) is limited to data obtained downstream of "natural" transition; category 2 (Fig. 2) is limited to nozzle wall data where laminarization and retransition did not occur along the nozzle wall (i.e., transition occurred far upstream of the measuring station).

Several conclusions can readily be drawn from the results shown on Figs. 1 and 2. Within the scatter of the data on Fig. 1 (which is considerable, due partly to inaccuracies in determining C_f, N, etc) there is a definite increase in $(\ell/\delta)_m$ at low Reynolds numbers *which is essentially independent of Mach number, T_w/T_t, and γ* (although there is a slight trend of decreasing $(\ell/\delta)_m$ with decreasing wall temperatures). Comparison of Figs. 1 and 2 strongly indicates that the low Reynolds number amplification of $(\ell/\delta)_m$ results from transitional flow structure because the nozzle wall data, where transition occurred far upstream of the measuring station, do not exhibit the increase in $(\ell/\delta)_m$ at low Reynolds number. This conclusion supports the results of Ref. 19, where low values of $(\ell/\delta)_m$ were needed to compute low Reynolds number flow on a swept leading edge (where transition occurred near the tip). Sufficient data do not exist to conclude whether or not the influence of a strong transition trigger would persist beyond the "end" of transition, but because the amplification at low Reynolds number is a result of the transitional flow structure such a possibility is strongly suggested.

Where laminarization and retransition occur along a nozzle wall, as in the $M=20$, 22-in. helium data[5] and in Ref. 69 of Ref. 7 at Mach number approximately 4-5, a large amplification of $(\ell/\delta)_m$ is again observed, although these data are not shown herein. Thus, the observed amplification in $(\ell/\delta)_m$ at low Reynolds number is a function of proximity to transition, in agreement with Ref. 7 where the N-overshoot was shown to depend upon the profile location in terms of boundary-layer thicknesses downstream of transition. Some of the scatter in Fig. 1 may result from the fact that the relative location to transition is not directly included in δ^+. A further conclusion from Figs. 1 and 2 is that a δ^+ value of $\simeq$ 2,000 provides a convenient criteria for defining a "fully developed" ($dp/dx \simeq 0$), turbulent boundary layer over a wide range of Mach number and wall temperature.

These conclusions lead to a rather interesting consequence regarding the importance of transition location. For a hypersonic cruise vehicle at Mach 10, with wall to total temperature ratio $=0.2$ and at 130,000 ft cruise altitude, a δ^+ value of 2000 corresponds to a distance of $\simeq$ 60-80 ft back along the fuselage. Therefore the low Reynolds number boundary layer, which has considerable application at low speeds (such as turbine blades, etc.) is even more important as Mach number is increased.[20]

The present results indicate that the structure of low Reynolds number turbulent wall flows is not unique but is a function of the proximity to transition and perhaps of the type of transitional flow as well (i.e., violently triggered vs "natural"). This implies that a knowledge of transition location may be of considerable importance to the design of high speed vehicles. The present results also indicate that nozzle wall data have a low Reynolds number simulation problem as well as the wall temperature and pressure gradient history effects already documented.[5,9,21]

References

[1] McDonald, H., "Mixing Length and Kinematic Eddy Viscosity in a Low Reynolds Number Boundary Layer," Rept. J214453-1, Sept. 1970, Research Lab., United Technologies Corp., East Hartford, Conn.

[2] Cebeci, Tuncer, "A Model for Eddy-Conductivity and Turbulent Prandtl Number," Rept. MDC-J747/01, May 1970, McDonnell Douglas Corp., Huntington Beach, Calif.

[3] Simpson, Roger L., "Characteristics of Turbulent Boundary Layers at Low Reynolds Numbers With and Without Transporation," *Journal of Fluid Mechanics*, Vol. 42, Pt. 4, July 30, 1970, pp. 769-802.

[4] Baker, R. J. and Launder, B. E., "The Turbulent Boundary Layer with Foreign Gas Injection—I. Measurements in Zero Pressure Gradient," *International Journal of Heat Mass Transfer*, Vol. 17, Pergamon Press, New York, 1974, pp. 275-291.

[5] Bushnell, Dennis M. and Morris, Dana J., "Shear-Stress, Eddy-Viscosity, and Mixing-Length Distributions in Hypersonic Turbulent Boundary Layers," TM X-2310, Aug. 1971, NASA.

[6] Bushnell, D. M. and Alston, D. W., "Calculation of Transitional Boundary-Layer Flows," *AIAA Journal*, Vol. 11, April 1973, pp. 554-556.

[7] Johnson, C. B. and Bushnell, D. M., "Power Law Velocity-Profile-Exponent Variations with Reynolds Number, Wall Cooling, and Mach Number in a Turbulent Boundary Layer," TN D-5753, April 1970, NASA.

[8] Sandborn, V. A., "A Review of Turbulence Measurements in Compressible Flow," TM X-62,337, March 1974, NASA.

[9] Bushnell, D. M., Johnson, C. B., Harvey, W. D., and Feller, W. V., "Comparison of Prediction Methods and Studies of Relaxation in Hypersonic Turbulent Nozzle-Wall Boundary Layers," TN D-5433, Sept. 1969, NASA.

[10] Watson, R. D., Harris, J. E., and Anders, J. B., Jr., "Measurements in a Transitional/Turbulent Mach 10 Boundary Layer at High Reynolds Numbers," AIAA Paper 73-165, Washington, D.C., 1974.

[11] Fischer, M. C. and Maddalon, D. V., "Experimental Laminar, Transitional, and Turbulent Boundary-Layer Profiles on a Wedge at Local Mach Number 6.5 and Comparisons with Theory," TN D-6462, Sept. 1971, NASA.

[12] Hastings, R. C. and Sawyer, W. G., "Turbulent Boundary Layers on a Large Flat Plate at $M=4$," R&M, 3678, March 1970, Aerodynamics Dept., Royal Aircraft Establishment, Farnborough, Hants, U.K.

[13] Hopkins, E. J., Keener, E. R., and Dwyer, H. A. "Turbulent Skin Friction and Boundary-Layer Profiles Measured on Nonadiabatic Flat Plates at Hypersonic Mach Numbers," *AIAA Journal*, Vol. 10, Jan. 1972, pp. 40-48.

[14] Keener, E. R. and Hopkins, E. J., "Turbulent Boundary-Layer Velocity Profiles on a Nonadiabatic Flat Plate at Mach Number 6.5," TN D-6907, Aug. 1972, Aug. 1972, NASA.

[15] Beckwith, I. E., Harvey, W. D., and Clark, F. L., "Comparisons of Turbulent-Boundary-Layer Measurements at Mach Number 19.5 With Theory and an Assessment of Probe Errors," TN D-6192, June 1971, NASA.

[16] Winter, K. G. and Gaudet, L., "Turbulent Boundary-Layer Studies at High Reynolds Numbers at Mach Numbers between 0.2 and 2.8," R&M 3712, Dec. 1970, Aerodynamics Dept., Royal Aircraft Establishment, Farnborough, Hants, U.K.

[17] Sivasegaram, S. and Whitelaw, J. H., "The Prediction of Turbulent, Supersonic, Two-Dimensional, Boundary-Layer Flows," *The Aeronautical Quarterly*, Jan. 1970, pp. 274-294.

[18] Squire, L. C., "Eddy Viscosity Distributions in Compressible Turbulent Boundary Layers with Injection," *The Aeronautical Quarterly*, Vol. XXIII, May 1971, pp. 168-182.

[19] Hunt, J. L. Bushnell, D. M., and Beckwith, I. E., "The Compressible Turbulent Boundary Layer on a Blunt Swept Slab With and Without Leading-Edge Blowing," TN D-6203, March 1971, NASA.

[20] Morkovin, M. V., "Effects of Compressibility on Turbulent Flows," *The Mechanics of Turbulence*, Aug.-Sept. 1961, Gordon and Breach, Marseille, France.

[21] Gates, D., "An Experimental Investigation of the Effect of Upstream Conditions on the Downstream Characteristics of Compressible Turbulent Boundary Layers," Ph.D. thesis, 1973, Dept. of Mechanical Engineering, University of Maryland, College Park, Md.

[22] Spalding, D. B. and Chi, S. W., "The Drag of a Compressible Turbulent Boundary Layer on a Smooth Flat Plate With and Wihout Heat Transfer," *Journal of Fluid Mechanics*, Vol. 18, Pt. 1, Jan. 1964, pp. 117-143.

[23] Bertram, M. H. and Neal, L. Jr., "Recent Experiments in Hypersonic Turbulent Boundary Layers," TM X-56335, May 1965, NASA.